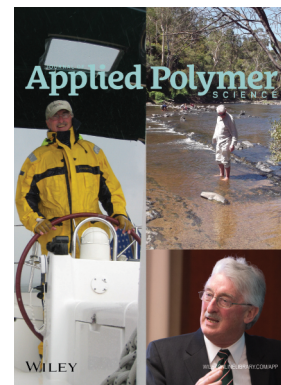


Special Issue: Sustainable Polymers and Polymer Science
Dedicated to the Life and Work of Richard P. Wool

Guest Editors: Dr Joseph F. Stanzione III (Rowan University, U.S.A.)
and Dr John J. La Scala (U.S. Army Research Laboratory, U.S.A.)



EDITORIAL

Sustainable Polymers and Polymer Science: Dedicated to the Life and Work of Richard P. Wool
Joseph F. Stanzione III and John J. La Scala, *J. Appl. Polym. Sci.* 2016, DOI: [10.1002/app.44212](https://doi.org/10.1002/app.44212)

REVIEWS

Richard P. Wool's contributions to sustainable polymers from 2000 to 2015
Alexander W. Bassett, John J. La Scala and Joseph F. Stanzione III, *J. Appl. Polym. Sci.* 2016,
DOI: [10.1002/app.43801](https://doi.org/10.1002/app.43801)

Recent advances in bio-based epoxy resins and bio-based epoxy curing agents
Elyse A. Baroncini, Santosh Kumar Yadav, Giuseppe R. Palmese and Joseph F. Stanzione III, *J. Appl. Polym. Sci.* 2016,
DOI: [10.1002/app.44103](https://doi.org/10.1002/app.44103)

Recent advances in carbon fibers derived from bio-based precursors
Amod A. Ogale, Meng Zhang and Jing Jin, *J. Appl. Polym. Sci.* 2016, DOI: [10.1002/app.43794](https://doi.org/10.1002/app.43794)

RESEARCH ARTICLES

Flexible polyurethane foams formulated with polyols derived from waste carbon dioxide
Mica DeBolt, Alper Kiziltas, Deborah Mielewski, Simon Waddington and Michael J. Nagridge, *J. Appl. Polym. Sci.* 2016,
DOI: [10.1002/app.44086](https://doi.org/10.1002/app.44086)

Sustainable polyacetals from erythritol and bioaromatics
Mayra Rostagno, Erik J. Price, Alexander G. Pemba, Ion Ghiriviga, Khalil A. Abboud and Stephen A. Miller, *J. Appl. Polym. Sci.*
2016, DOI: [10.1002/app.44089](https://doi.org/10.1002/app.44089)

Bio-based plasticizer and thermoset polyesters: A green polymer chemistry approach
Mathew D. Rowe, Ersan Eyiler and Keisha B. Walters, *J. Appl. Polym. Sci.* 2016, DOI: [10.1002/app.43917](https://doi.org/10.1002/app.43917)

The effect of impurities in reactive diluents prepared from lignin model compounds on the properties of vinyl ester resins
Alexander W. Bassett, Daniel P. Rogers, Joshua M. Sadler, John J. La Scala, Richard P. Wool and Joseph F. Stanzione III,
J. Appl. Polym. Sci. 2016, DOI: [10.1002/app.43817](https://doi.org/10.1002/app.43817)

Mechanical behaviour of palm oil-based composite foam and its sandwich structure with flax/epoxy composite
Siew Cheng Teo, Du Ngoc Uy Lan, Pei Leng Teh and Le Quan Ngoc Tran, *J. Appl. Polym. Sci.* 2016, DOI: [10.1002/app.43977](https://doi.org/10.1002/app.43977)

Mechanical properties of composites with chicken feather and glass fibers
Mingjiang Zhan and Richard P. Wool, *J. Appl. Polym. Sci.* 2016, DOI: [10.1002/app.44013](https://doi.org/10.1002/app.44013)

Structure–property relationships of a bio-based reactive diluent in a bio-based epoxy resin
Anthony Maiorana, Liang Yue, Ica Manas-Zloczower and Richard Gross, *J. Appl. Polym. Sci.* 2016, DOI: [10.1002/app.43635](https://doi.org/10.1002/app.43635)

Bio-based hydrophobic epoxy-amine networks derived from renewable terpenoids
Michael D. Garrison and Benjamin G. Harvey, *J. Appl. Polym. Sci.* 2016, DOI: [10.1002/app.43621](https://doi.org/10.1002/app.43621)

Dynamic heterogeneity in epoxy networks for protection applications
Kevin A. Masser, Daniel B. Knorr Jr., Jian H. Yu, Mark D. Hindenlang and Joseph L. Lenhart, *J. Appl. Polym. Sci.* 2016,
DOI: [10.1002/app.43566](https://doi.org/10.1002/app.43566)

Special Issue: Sustainable Polymers and Polymer Science
Dedicated to the Life and Work of Richard P. Wool

Guest Editors: Dr Joseph F. Stanzione III (Rowan University, U.S.A.)
and Dr John J. La Scala (U.S. Army Research Laboratory, U.S.A.)

Statistical analysis of the effects of carbonization parameters on the structure of carbonized electrospun organosolv lignin fibers

Vida Poursorkhabi, Amar K. Mohanty and Manjusri Misra, *J. Appl. Polym. Sci.* 2016, DOI: 10.1002/app.44005

Effect of temperature and concentration of acetylated-lignin solutions on dry-spinning of carbon fiber precursors

Meng Zhang and Amod A. Ogale, *J. Appl. Polym. Sci.* 2016, DOI: 10.1002/app.43663

Poly(lactic acid) bioconjugated with glutathione: Thermosensitive self-healed networks

Dalila Djidi, Nathalie Mignard and Mohamed Taha, *J. Appl. Polym. Sci.* 2016, DOI: 10.1002/app.43436

Sustainable biobased blends from the reactive extrusion of polylactide and acrylonitrile butadiene styrene

Ryan Vadori, Manjusri Misra and Amar K. Mohanty, *J. Appl. Polym. Sci.* 2016, DOI: 10.1002/app.43771

Physical aging and mechanical performance of poly(L-lactide)/ZnO nanocomposites

Erlantz Lizundia, Leyre Pérez-Álvarez, Míriam Sáenz-Pérez, David Patrocínio, José Luis Vilas and Luis Manuel León, *J. Appl. Polym. Sci.* 2016, DOI: 10.1002/app.43619

High surface area carbon black (BP-2000) as a reinforcing agent for poly[(-)-lactide]

Paula A. Delgado, Jacob P. Brutman, Kristina Masica, Joseph Molde, Brandon Wood and Marc A. Hillmyer, *J. Appl. Polym. Sci.* 2016, DOI: 10.1002/app.43926

Encapsulation of hydrophobic or hydrophilic iron oxide nanoparticles into poly-(lactic acid) micro/nanoparticles via adaptable emulsion setup

Anna Song, Shaowen Ji, Joung Sook Hong, Yi Ji, Ankush A. Gokhale and Ilsoon Lee, *J. Appl. Polym. Sci.* 2016, DOI: 10.1002/app.43749

Biorenewable blends of polyamide-4,10 and polyamide-6,10

Christopher S. Moran, Agathe Barthelon, Andrew Pearsall, Vikas Mittal and John R. Dorgan, *J. Appl. Polym. Sci.* 2016, DOI: 10.1002/app.43626

Improvement of the mechanical behavior of bioplastic poly(lactic acid)/polyamide blends by reactive compatibilization

JeongIn Gug and Margaret J. Sobkowicz, *J. Appl. Polym. Sci.* 2016, DOI: 10.1002/app.43350

Effect of ultrafine talc on crystallization and end-use properties of poly(3-hydroxybutyrate-co-3-hydroxyhexanoate)

Jens Vandewijngaarden, Marius Murariu, Philippe Dubois, Robert Carleer, Jan Yperman, Jan D'Haen, Roos Peeters and Mieke Buntinx, *J. Appl. Polym. Sci.* 2016, DOI: 10.1002/app.43808

Microfibrillated cellulose reinforced non-edible starch-based thermoset biocomposites

Namrata V. Patil and Anil N. Netravali, *J. Appl. Polym. Sci.* 2016, DOI: 10.1002/app.43803

Semi-IPN of biopolyurethane, benzyl starch, and cellulose nanofibers: Structure, thermal and mechanical properties

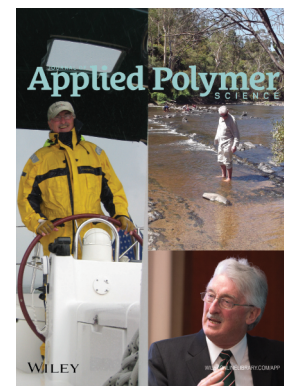
Md Minhaz-Ul Haque and Kristiina Oksman, *J. Appl. Polym. Sci.* 2016, DOI: 10.1002/app.43726

Lignin as a green primary antioxidant for polypropylene

Renan Gadioli, Walter Ruggeri Waldman and Marco Aurelio De Paoli *J. Appl. Polym. Sci.* 2016, DOI: 10.1002/app.43558

Evaluation of the emulsion copolymerization of vinyl pivalate and methacrylated methyl oleate

Alan Thyago Jensen, Ana Carolina Couto de Oliveira, Sílvia Belém Gonçalves, Rossano Gambetta and Fabricio Machado *J. Appl. Polym. Sci.* 2016, DOI: 10.1002/app.44129



Sustainable polyacetals from erythritol and bioaromatics

Mayra Rostagno, Erik J. Price, Alexander G. Pemba, Ion Ghiriviga, Khalil A. Abboud, Stephen A. Miller

The George and Josephine Butler Laboratory for Polymer Research, Department of Chemistry, University of Florida, Gainesville, Florida 32611-7200

Correspondence to: S. A. Miller (E-mail: miller@chem.ufl.edu)

ABSTRACT: The polymerization of biorenewable molecules to polymers with hydrolyzable main-chain functionality is one approach to identifying sustainable replacements for common, environmentally unsound packaging plastics. Bioaromatic polyacetals were synthesized via acid-catalyzed acetal formation from dialdehydes and tetraols. Ethylene linked dialdehyde monomers **VV** and **SS** were constructed from bioaromatics vanillin and syringaldehyde, respectively. Tetraol monomers included biogenic erythritol (**E**), along with pentaerythritol (**P**), and ditrimethylolpropane (**D**). Four copolymer series were prepared with varying tetraol content: **E/P-VV**; **E/D-VV**; **E/P-SS**; and **E/D-SS**. Number average molecular weights (M_n) ranged from 1,400 to 27,100 Da. Generally, the copolymerization yields were inversely proportional to the feed fraction of erythritol (**E**), implying that tetraols **P** and **D** react more readily. The materials were typically amorphous and exhibited glass transition temperatures (T_g) ranging from 57 to 159 °C, suitably mimicking the T_g values of several commodity plastics. The syringaldehyde-based copolymers exhibited a higher T_g range (71–159 °C) than the vanillin-based copolymers (57–110 °C). Accelerated degradation studies in aqueous HCl (3 M, 6 M, concentrated) over 24 h showed that degradation (M_n decrease) was proportional to the acid concentration. A one-year degradation study of **E50/D50-SS** (from 50% feed of erythritol) in seawater, deionized water, tap water, or pH 5 buffer showed no M_n decrease; but in pH 1 buffer, the decrease was 40% (18,800 to 11,200). © 2016 Wiley Periodicals, Inc. *J. Appl. Polym. Sci.* **2016**, *133*, 44089.

KEYWORDS: biodegradable; biopolymers and renewable polymers; cellulose and other wood products; degradation; thermal properties

Received 20 January 2016; accepted 7 June 2016

DOI: 10.1002/app.44089

INTRODUCTION

Petroleum and natural gas resources for commodity plastic manufacturing are not indefinitely guaranteed.¹ Moreover, worldwide plastic production is ever increasing while recycling efforts are stagnant.² These two factors highlight the need to invent and produce renewable polymers that possess inherent degradability. Applying the Principles of Green Chemistry³ to the enormous commodity plastics industry seems to be necessary for the ultimate preservation of the planet and the quality of life of its inhabitants. Two pertinent Principles of Green Chemistry are #7, “use of renewable feedstocks”—as illustrated by the epitomic research of Professor Wool⁴—as well as #10, “design for degradation.” Properly applied, these two Principles could transform the plastics industry from environmentally perilous to sustainable.

Perhaps the most successful green polymer is polylactic acid (PLA),^{5–7} pioneered by NatureWorks in Blair, Nebraska⁸ where cornstarch is converted to glucose, then to lactic acid, then to lactide, which is subject to ring-opening polymerization. The Nebraska capacity is about 1.4×10^8 kg/year, which is roughly

1/3 of worldwide PLA production⁹ and is about 1/1000 the volume of worldwide polyolefin production.¹⁰ The majority of this plastic is targeted for food packaging applications, especially as a replacement for polystyrene (PS). PLA possesses several admirable qualities, including good optical transparency, low residual color, and good dimensional stability.^{5,11} However, its low glass transition temperature ($T_g = 55$ °C) will probably prevent it from completely replacing petroleum-based PS ($T_g = 100$ °C)¹² and becoming a universal packaging thermoplastic. Moreover, PLA is inherently brittle,¹³ exhibits poor barrier properties,¹⁴ and composts very slowly under typical environmental conditions.^{15–18} The claim of “compostable” reportedly only applies to municipal/industrial composting facilities.^{19,20}

Our research group designs and synthesizes new polymers based on biorenewable feedstocks, while targeting higher glass transition temperatures and improved degradation behavior. This manuscript describes our synthesis of novel polyacetals built from lignin-based bioaromatics and tetraols, including erythritol, a naturally occurring polyol (sugar alcohol).

Additional Supporting Information may be found in the online version of this article.

© 2016 Wiley Periodicals, Inc.

Erythritol is of special interest since it is a biogenic tetraol and can be found in fruits and fermented foods. Commercially, it is produced via the fermentation of glucose²¹ and has been approved by the U.S. Food and Drug Administration for human consumption as a low-calorie sweetener, among other uses.²² There are a few literature examples of erythritol employed for polymer synthesis: as a branching molecule in star polymers^{23,24}; for modification with azide for “click” chemistry polymers²⁵; and for aliphatic polyester preparation by selective reaction through the two primary alcohols, providing amorphous materials with T_g values below 0 °C.²⁶ This is the first report of erythritol used for preparing fully biorenewable, linear polymers exhibiting good thermal properties. We previously reported the synthesis of aromatic polyacetals with alternative tetraols ditrimethylolpropane and pentaerythritol.²⁷ Even though these are not naturally occurring molecules, pathways exist for their synthesis via fermentation and renewable C1 feedstocks.

The bioaromatics investigated herein are vanillin and syringaldehyde.²⁸ Although 85% of commercial vanillin is synthesized through petrochemical routes, about 15% is produced from softwood forestry lignin waste alongside refined cellulose at paper mills.²⁹ Syringaldehyde, bearing one additional methoxy group, is also available from lignin, although it is found in greater abundance in hardwood lignin.^{30,31} While the demand for syringaldehyde is much lower and it is largely a petroleum-based product, it is also produced by lignin oxidation.³²

The utilization of aromatic moieties to improve material properties has been extensively applied in the field of polymers. PS has a high T_g (100 °C),¹² conferred by pendent phenyl rings, which increase conformational barriers and allow for π stacking—thereby promoting structural rigidity. Meanwhile, polyethylene terephthalate (PET) has a high melting temperature (265 °C)³³ due, in part, to main chain aromaticity. Increasing polymeric T_g and T_m with aromatics has also been achieved in the field of renewable polymers—prominently with vanillin.³⁴ This versatile bioaromatic has been converted into a styrene analogue³⁵ by esterification with methyl methacrylate, obtaining glass transition temperatures up to 120 °C. Vanillin has also been made into a polyacrylamide, achieving a competitive T_g of 101 °C.³⁶ Designed as PET analogues, polyalkylenehydroxybenzoates were obtained by condensing biobased aromatic hydroxyacids, including vanillic acid, with methylene spacers.³⁷ Finally, many renewable linear polymers have also been synthesized by transforming vanillin and its derivatives (vanillic alcohol and vanillic acid) into symmetrical, bifunctional monomers. The prime example is enzymatically obtained *bis-vanillin*. This biaryl dialdehyde was reacted with diamines to make polyaldimines,³⁸ made into polyesters by oxidation or reduction followed by copolymerization with aliphatic diols or diacids, respectively,³⁹ and extended to dialkenes to make polyesters via ADMET.⁴⁰ Polyesters were also made from vanillin derivatives vanillin alcohol and vanillic acid, the first via ADMET⁴¹ and the second via thiol-ene chemistry.⁴² Finally, vanillin bisphenols were prepared via McMurry coupling, reduced, and then converted into polycarbonates with T_g values near 86 °C.⁴³ Except for the polyaldimines, the aldehyde functional group of vanillin was either

oxidized or reduced prior to polymerization. Two recent review articles cover many more examples of vanillin incorporated into renewable polymers, including crosslinked and thermoset polymers.^{44,45}

A few examples of sustainable polyacetals exist in the literature. Semicrystalline aliphatic polyacetals obtained from formaldehyde equivalents and renewable diols were found to have low T_g and moderate T_m , which might make them adequate polyethylene mimics.^{46,47} Polyacetal thermal properties were improved by the incorporation of rigid rings from isosorbide, but it was found that the highest T_g values were obtained from using a non-naturally occurring stereoisomer.⁴⁸ Other novel polyacetals with rigid rings include thermoplastic polyurethanes incorporating pentaerythritol,⁴⁹ and poly(2,5-dihydroxy-1,4-dioxane) from the polymerization of glycoaldehyde dimer.⁵⁰

In this study, polyacetals are synthesized from aromatic dialdehydes and are targeted because of their anticipated hydrolysis in acidic media. Thus, degradability is conferred to the polymers by design. The library of sustainable, aromatic, and degradable polymers is expanded with the use of biogenic erythritol, affording polymers with good thermal properties. Detailed studies reveal the structure and stereochemistry of the incorporated erythritol moiety. Polymer and copolymer structure/property relationships are analyzed regarding the nature of the tetraol and the substituents present on the bioaromatics. Finally, preliminary degradation results are presented demonstrating the hydrolysis of polyacetals built with erythritol.

EXPERIMENTAL

Materials

Potassium iodide, phosphorus pentoxide, reagent grade methanol, reagent grade dichloromethane, reagent grade water, and sodium hydroxide were purchased from Fisher Scientific and used without further purification. Benzene was purchased from EMD and was utilized without further purification. Vanillin (from *Picea abies*, Norway spruce) was purchased from Borregaard Industries Ltd. and was utilized without further purification. Syringaldehyde, *para*-toluenesulfonic acid, benzaldehyde, and 1,2-dibromoethane were purchased from Sigma Aldrich and were utilized without further purification. Ditrimethylolpropane (di-TMP) was purchased from Sigma Aldrich and triturated in toluene before use. Pentaerythritol was purchased from Acros Organics and was recrystallized from a dilute aqueous HCl solution. Erythritol was purchased from Now Foods (100%, Item#: 6923) and utilized without further purification. NMR solvent deuterated dimethylsulfoxide (DMSO- d_6) was purchased from Cambridge Isotope Laboratories. Activated 4 Å molecular sieves, from Sigma Aldrich, were used to keep the NMR solvents dry. All other chemicals, unless noted otherwise, were used as received.

Characterization

Proton nuclear magnetic resonance (¹H-NMR) and carbon nuclear magnetic resonance spectra (¹³C-NMR) were recorded using an Inova 500 MHz spectrometer. Chemical shifts are reported in parts per million (ppm) downfield relative to tetramethylsilane (0.0 ppm) or residual proton in the specified

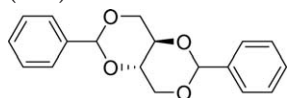
solvent. Coupling constants (J) are reported in Hertz (Hz). Multiplicities are reported using the following abbreviations: s, singlet; d, doublet; t, triplet; q, quartet; m, multiplet; br, broad. Differential scanning calorimetry thermograms were obtained with a DSC Q1000 from TA instruments. Typically, 1.5–3 mg of a sample was massed and added to a sealed pan that passed through a heat/cool/heat cycle at 10 °C/min. Reported data are from the second full cycle. The temperature ranged from 0 to 180 °C. Thermogravimetric analyses were measured under nitrogen with a TGA Q5000 (TA Instruments). About 5–10 mg of each sample were heated at 20 °C/min from 25 to 600 °C. Gel permeation chromatography (GPC) was performed at 40 °C using an Agilent Technologies 1260 Infinity Series liquid chromatography system with an internal differential refractive index detector, and two Waters Styragel HR-5E columns (7.8 mm i.d., 300 mm length, guard column 7.8 mm i.d., 25 mm length) using a solution of 0.1% potassium triflate (K[OTf]) in HPLC grade hexafluoroisopropanol (HFIP) as the mobile phase at a flow rate of 0.5 mL/min. Calibration was performed with narrow polydispersity polymethyl methacrylate (PMMA) standards. X-ray intensity data were collected at 100 K on a Bruker DUO diffractometer using MoK α radiation ($\lambda = 0.71073$ Å) and an APEXII CCD area detector. Raw data frames were read by program SAINT1 and integrated using 3D profiling algorithms. The resulting data were reduced to produce hkl reflections and their intensities and estimated standard deviations. The data were corrected for Lorentz and polarization effects and numerical absorption corrections were applied based on indexed and measured faces. The structure was solved and refined in SHELXTL2013, using full-matrix least-squares refinement. The non-H atoms were refined with anisotropic thermal parameters and all of the H atoms were calculated in idealized positions and refined riding on their parent atoms. The molecules are located on inversion centers; thus, a half molecule exists in the asymmetric unit. In the final cycle of refinement, 1665 reflections [of which 1322 are observed with $I > 2\sigma(I)$] were used to refine 100 parameters and the resulting R_1 , wR_2 , and S (goodness of fit) were 3.90%, 10.35%, and 1.101, respectively. The refinement was carried out by minimizing the wR_2 function using F^2 rather than F values. R_1 is calculated to provide a reference to the conventional R value but its function is not minimized.

Monomer Preparation

Monomer preparations were similar to our previously reported methods²⁷ and are detailed in the Supporting Information.

Model Compound Preparation

(4aR,8aS)-2,6-Diphenyltetrahydro-[1,3]Dioxino[5,4-d][1,3]Dioxine (BEB)



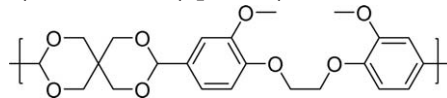
A 100 mL round bottom flask was charged with 1.22 g (10 mmol, 1 eq.) of erythritol, 2.65 g (25 mmol, 2.5 eq.) of benzaldehyde, 38 mg (2 mol %, 0.2 mmol) of *p*-TSA, and 50 mL of benzene. The flask was then fitted with a Dean-Stark trap and a reflux condenser, and then left to reflux overnight. The excess

benzene was removed by rotary evaporation leaving behind the crude product as an amorphous solid. The product was purified by two recrystallizations from minimal amounts of ethanol and isolated as a white crystalline solid in 50.3% yield (1.50 g). ¹H NMR (DMSO- d_6) δ ppm 3.92 (m, 4 H), 4.26 (dd, $J = 9.7, 3.4$ Hz, 2 H), 5.79 (s, 2 H), 7.38 (m, 6 H), 7.43 (m, 4 H). ¹³C NMR (DMSO- d_6) δ ppm 67.8, 73.1, 101.0, 126.1, 128.1, 128.9, 137.5. To prepare crystals for X-ray crystallography, 50 mg of **BEB** were placed in a scintillation vial and dissolved in minimal amounts of THF, and then allowed to stand. After a few days, as the solvent evaporated, crystals of **BEB** formed at the bottom of the vial. Analogous model compounds built from vanillin (**VEV**) and syringaldehyde (**SES**) were prepared in a similar manner (see the Supporting Information), but could not be grown into crystals suitable for X-ray diffraction analysis.

Polymer Synthesis

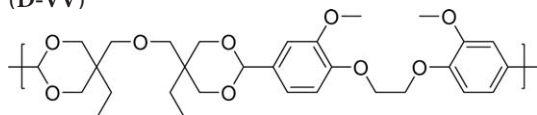
Four series of polymers were synthesized, where erythritol (**E**) was combined with a second tetraol [pentaerythritol (**P**) or ditrimethylolpropane (**D**)] and a dialdehyde (**VV** or **SS**). Two copolymer series employing **VV** were synthesized using an **E** feed % of 100, 90, 80, 60, 50, 40, 20, and 0 (molar percentage); the balance tetraol was either **P** or **D**. Two copolymer series employing **SS** were synthesized using an **E** feed % of 100, 90, 80, 70, 60, 50, 40, 30, 20, 10, and 0 (molar percentage); the balance tetraol was either **P** or **D**. Procedures for the polymers made from a single tetraol (**P-VV**; **D-VV**; **E-VV**; **P-SS**; **D-SS**; **E-SS**) are described below, along with a typical procedure for each copolymer series containing two tetraols. Detailed information for quantities of reagents used, obtained yields, and erythritol incorporation can be found in the Supporting Information.

Synthesis of Poly(pentaerythritol-co-VV) (P-VV)



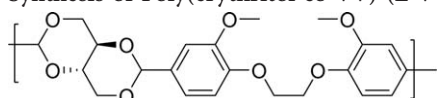
VV (0.660 g, 2 mmol), 0.270 g (2 mmol) of pentaerythritol (**P**), 4 mg (1 mol %) *p*-TSA, and 10 mL of dichloromethane were added to a 25 mL drop-shaped flask. The flask was fitted with a reflux condenser and the reaction was refluxed under a nitrogen atmosphere for 48 h. P_2O_5 was placed in the condenser to sequester the water that was produced as a by-product, and was replaced on demand (usually 4 times) during the reaction to prevent H_3PO_4 from leaking into the flask. The solution was poured into 150 mL cold basic methanol. The polymer precipitated as a powdery white solid. The product was obtained in 84.8% yield (0.73 g). ¹H NMR (DMSO- d_6) δ ppm 3.65 (d, $J = 11.4$ Hz, 2 H), 3.77 (m, 6H), 3.77 (d, 2H), 3.88 (d, $J = 10.7$ Hz, 2 H), 4.28 (s, 4H), 4.58 (d, $J = 11.4$ Hz, 2 H), 5.44 (s, 2H), 6.99 (m, 6H). ¹³C NMR (DMSO- d_6) δ ppm 32.0, 55.4, 55.5, 61.1, 66.9, 67.1, 67.4, 70.0, 101.2, 109.8, 109.9, 112.3, 112.56, 112.65, 118.6, 126.0, 129.9, 131.5, 148.0, 148.5, 149.2, 153.2, 191.4. Note that the four methylene carbons connected to the spiro carbon are inequivalent as confirmed by the splitting found in the ¹H NMR spectra.

Synthesis of Poly(ditrimethylolpropane-co-VV) (D-VV)



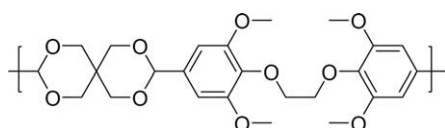
This polymer was synthesized using the same procedure as for **P-VV**; 0.660 g (2 mmol) of **VV**, 0.501 g (2 mmol) of ditrimethylolpropane (**D**), 4 mg (1 mol %) *p*-TSA, and 10 mL of dichloromethane were used. The polymer precipitated as an amorphous solid that hardened upon drying. The product was obtained in 92.6% yield (1.01 g). ^1H NMR (DMSO- d_6) δ ppm 0.79, 0.88 (m, 6H); 1.18, 1.76 (m, 4H), 3.27, 3.30 (m, 1H), 3.58 (m, 4H), 3.69 (s, 3H), 3.71 (m, 3H), 3.73 (s, 3H), 3.85 (m, 1H), 3.95 (m, 3H), 4.24 (s, 4H), 5.35 (s, 2H), 6.96 (m, 6H). ^{13}C NMR (DMSO- d_6) δ ppm 6.8, 7.6, 7.8, 23.1, 23.9, 36.1, 36.3, 36.7, 54.9, 55.3, 55.4, 67.11, 70.2, 71.4, 71.7, 100.79, 100.85, 110.0, 112.6, 118.5, 131.8, 148.0, and 148.5. Because of the stereoirregularity of the polymer, multiple peaks are observed in both the ^1H and ^{13}C NMR spectra. Some peaks are coincident and therefore cannot be distinguished from one another.

Synthesis of Poly(erythritol-co-VV) (E-VV)



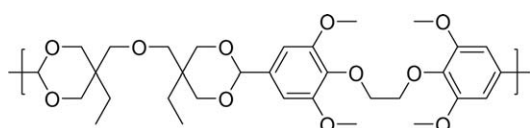
This polymer was synthesized using the same procedure as for **P-VV**. 0.660 g (2 mmol) of **VV**, 0.244 g (2 mmol) of erythritol (**E**), 4 mg (1 mol %) *p*-TSA, and 10 mL of dichloromethane were used. The polymer precipitated as a powdery solid. The product was obtained in 46.1% yield (0.383 g). ^1H NMR (DMSO- d_6) δ ppm 3.75 (s, 6 H), 3.83 (m, 2 H), 4.08 (m, 1 H), 4.32 (m, 6 H), 4.43 (m, 1 H), 5.72, 5.87 (m, 2 H), 7.01 (m, 6 H). The ^{13}C NMR spectra could not be obtained due to the low solubility of the polymer in DMSO- d_6 .

Synthesis of Poly(pentaerythritol-co-SS) (P-SS)



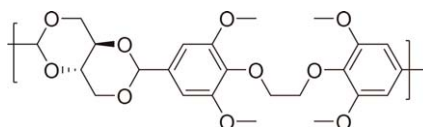
This polymer was synthesized using the same procedure as for **P-VV**; 0.780 g (2 mmol) of **SS**, 0.270 g (2 mmol) of pentaerythritol (**P**), 4 mg (1 mol %) *p*-TSA, and 10 mL of dichloromethane were used. The product was obtained in 88.7% yield (0.870 g). ^1H NMR (DMSO- d_6) δ ppm 3.63 (m, 2 H), 3.76 (s, 12 H), 3.79 (m, 2 H), 3.88 (d, $J=10.7$ Hz, 2 H), 4.08 (s, 4 H), 4.58 (d, $J=11.2$ Hz, 2 H), 5.43 (s, 2 H), 6.72 (m, 4 H). ^{13}C NMR (DMSO- d_6) δ ppm 32.5, 56.4, 69.9, 70.3, 70.5, 71.8, 101.5, 103.9, 134.4, 137.2, and 153.1.

Synthesis of Poly(ditrimethylolpropane-co-SS) (D-SS)



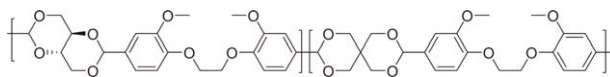
This polymer was synthesized using the same procedure as for **P-VV**. 0.780 g (2 mmol) of **SS**, 0.501 g (2 mmol) of ditrimethylolpropane (**D**), 4 mg (1 mol %) *p*-TSA, and 10 mL of dichloromethane were used. The product was obtained in 73.7% yield (0.890 g). ^1H NMR (DMSO- d_6) δ ppm 0.80, 0.88 (m, 6 H), 1.18, 1.75 (m, 4 H), 3.57, 3.70, 3.74, 3.86, 3.95 (m, 24 H), 4.07 (s, 4 H), 5.35 (s, 2 H), 6.68 (s, 4 H). ^{13}C NMR (DMSO- d_6) δ ppm 6.8, 7.8, 23.1, 23.76, 23.85, 36.2, 36.3, 36.7, 54.9, 55.79, 55.86, 70.0, 71.3, 71.4, 71.7, 100.65, 100.70, 103.4, 134.2, 136.6, 152.5, and 153.1. Because of the stereoirregularity of the polymer, multiple peaks are observed in both the ^1H and ^{13}C NMR spectra. Some peaks are coincident and therefore cannot be distinguished from one another.

Synthesis of Poly(erythritol-co-SS) (E-SS)



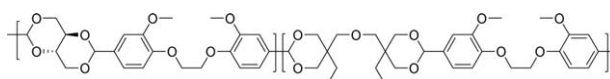
This polymer was synthesized using the same procedure as for **P-VV**; 0.780 g (2 mmol) of **SS**, 0.244 g (2 mmol) of erythritol (**E**), 4 mg (1 mol %) *p*-TSA, and 10 mL of dichloromethane were used. The polymer precipitated as a powdery solid. The product was obtained in 28.4% yield (0.270 g). ^1H NMR (DMSO- d_6) δ ppm 3.76 (m, 12 H), 3.90 (m, 2 H), 4.09 (br s, 4 H), 4.30 (m, 4 H), 5.71, 5.87 (m, 2 H), and 6.72 (m, 4 H). ^{13}C NMR spectra could not be obtained due to the low solubility of the polymer in DMSO- d_6 .

Synthesis of Poly(erythritol-co-pentaerythritol-co-VV) (E/P-VV) 60%E/40%P



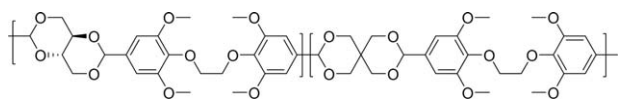
This polymer was synthesized using the same procedure as for **P-VV**. 0.661 g (2 mmol) of **VV**, 0.109 g (0.8 mmol) of pentaerythritol (**P**), 0.147 g (1.2 mmol) of erythritol (**E**), 4 mg (1 mol %) *p*-TSA, and 10 mL of dichloromethane were used. The polymer precipitated as a powdery white solid. The product was obtained in 90.6% yield (0.765 g). ^1H NMR (DMSO- d_6) δ ppm 3.65, 3.76, 4.07, 4.58 (m, 9.8 H), 3.88 (m, 2 H), 4.28 (m, 5 H), 5.43, 5.71, 5.87 (m, 2 H), 6.99 (m, 6 H). ^{13}C NMR (DMSO- d_6) δ ppm 32.0, 54.9, 55.2, 55.43, 55.46, 55.50, 60.7, 63.3, 66.7, 66.9, 67.1, 67.4, 67.5, 67.8, 69.5, 70.0, 70.8, 72.6, 73.1, 75.9, 76.1, 83.2, 100.1, 101.0, 101.2, 103.3, 103.6, 103.7, 109.8, 109.9, 110.2, 110.4, 110.5, 112.3, 112.4, 112.6, 112.7, 118.6, 118.7, 119.3, 119.5, 119.7, 126.0, 129.86, 129.94, 130.0, 130.5, 130.7, 131.5, 148.0, 148.1, 148.2, 148.4, 148.5, 148.67, 148.74, 149.2, 153.1, and 153.2. Note that the four methylene carbons connected to the spiro carbon are inequivalent as confirmed by the splitting found in the ^1H NMR spectra.

Synthesis of Poly(erythritol-co-ditrimethylolpropane-co-VV) (E/D-VV) 40%E/60%D



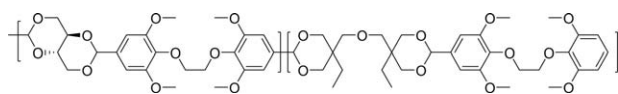
This polymer was synthesized using the same procedure as for **P-VV**. 0.660 g (2 mmol) of **VV**, 0.300 g (1.2 mmol) of ditrimethylolpropane (**D**), 0.098 g (0.8 mmol) of erythritol (**E**), 4 mg (1 mol %) *p*-TSA, and 10 mL of dichloromethane were used. The polymer precipitated as an amorphous solid that hardened upon drying. The product was obtained in 96.1% yield (0.948 g). ^1H NMR (DMSO- d_6) δ ppm 0.80, 0.89 (m, 3.6 H), 1.18, 1.76 (m, 2.4 H), 3.58, 3.69, 3.74, 3.90, 4.08, 4.39 (m, 15.6 H), 4.25 (s, 4H) 5.36, 5.70, 5.88 (m, 2 H), 6.97 (m, 6 H). ^{13}C NMR (DMSO- d_6) δ ppm 6.8, 7.9, 23.1, 23.8, 23.9, 36.2, 36.3, 36.7, 54.9, 55.3, 55.4, 55.5, 67.1, 67.8, 70.2, 70.3, 71.3, 71.4, 71.7, 71.9, 73.1, 75.9, 76.1, 100.1, 100.8, 100.9, 101.0, 109.9, 110.0, 110.2, 112.6, 118.49, 118.53, 118.7, 118.8, 119.2, 119.5, 119.7, 129.9, 130.5, 130.7, 131.8, 148.0, 148.1, 148.45, 148.47, 148.66, 148.73. Because of the stereoirregularity of the polymer, multiple peaks are observed in both the ^1H and ^{13}C NMR spectra. Some peaks are coincident and therefore cannot be distinguished from one another.

Synthesis of Poly(erythritol-co-pentaerythritol-co-SS) (E/P-SS) 50%E/50%P



This polymer was synthesized using the same procedure as for **P-VV**. 0.780 g (2 mmol) of **SS**, 0.136 g (1 mmol) of pentaerythritol (**P**), 0.122 g (1 mmol) of erythritol (**E**), 4 mg (1 mol %) *p*-TSA, and 10 mL of dichloromethane were used. The product was obtained in 82.0% yield (0.792 g). ^1H NMR (DMSO- d_6) δ ppm 3.65 (m, 2 H), 3.77 (m, 13 H), 3.88 (m, 2 H), 4.09 (s, 4 H), 4.31 (m, 1 H), 4.59 (d, $J = 11.7$ Hz, 1 H), 5.44, 5.72, 5.89 (m, 2 H), 6.73 (m, 4 H). ^{13}C NMR (DMSO- d_6) δ ppm 32.0, 55.9, 56.0, 63.3, 67.8, 69.4, 70.0, 71.3, 72.6, 73.1, 76.2, 100.1, 101.1, 103.4, 103.6, 133.9, 136.7, 152.6, 152.7, and 152.8. Because of the stereoirregularity of the polymer, multiple peaks are observed in both the ^1H and ^{13}C NMR spectra. Some peaks are coincident and therefore cannot be distinguished from one another.

Synthesis of Poly(erythritol-co-ditrimethylolpropane-co-SS) (E/D-SS) 50%E/50%D



This polymer was synthesized using the same procedure as for **P-VV**. 0.780 g (2 mmol) of **SS**, 0.250 g (1 mmol) of ditrimethylolpropane (**D**), 0.122 g (1 mmol) of erythritol (**E**), 4 mg (1 mol %) *p*-TSA, and 10 mL of dichloromethane were used. The product was obtained in 94.0% yield (1.02 g). ^1H NMR (DMSO- d_6) δ ppm 0.80, 0.88 (m, 3 H), 1.18, 1.74 (m, 2 H), 3.57 (m, 3 H), 3.66 (m, 1 H), 3.70, 3.75 (m, 12 H), 3.91 (m, 4H), 4.07 (s, 4H), 4.28 (m, 1H), 5.35, 5.69, 5.87 (m, 2 H), 6.68, 6.79, 6.85 (m, 4 H). ^{13}C NMR (DMSO- d_6) δ ppm 6.8, 7.8, 23.1, 23.9, 36.3, 36.7, 55.8, 55.9, 70.1, 71.3, 71.7, 73.1, 76.2, 100.65, 100.70, 100.1, 103.4, 103.6, 103.9, 104.4, 134.2, 136.6, 137.1, 152.5, 152.6, 152.7, 152.8, and 153.1. Because of the

stereoirregularity of the polymer, multiple peaks are observed for both the ^1H and ^{13}C NMR experiments. Some peaks are coincident and therefore cannot be distinguished from one another.

RESULTS AND DISCUSSION

Polymer Synthesis

Dialdehyde monomers were prepared in modest yields (51–54%) by reacting two equivalents of the biogenic hydroxyaldehydes vanillin (**V**) or syringaldehyde (**S**) with 1,2-dibromoethane, employing catalytic amounts of potassium iodide. The procedure is similar to our previous method²⁷ and provided suitable di-functional monomers (**VV** and **SS**) to polymerize with tetraols erythritol (**E**), pentaerythritol (**P**), and/or ditrimethylolpropane (**D**) to form polyacetals, as described in Figure 1 and Tables I–IV. Erythritol is a molecule that has two primary and two secondary alcohols, which seem to limit its reactivity compared to pentaerythritol and ditrimethylolpropane, which bear only primary alcohols. Accordingly, the polymers made from only erythritol are formed in comparatively low yield: **E-VV**, Table I, entry 8 with 46.1% yield; and **E-SS**, Table III, entry 26 with 28.4% yield. As shown in our previous work,²⁷ pentaerythritol and ditrimethylolpropane successfully formed polyacetals with aromatic dialdehydes. Thus, these more reactive tetraols are presumed to enable the “trapping” of erythritol into polyacetals via a copolymerization strategy—allowing for higher polymerization yields. Polymerization was achieved in solution using *p*-toluenesulfonic acid as the catalyst. Improved molecular weights were obtained by incorporating a drying agent in the system. Phosphorus pentoxide is a strong and irreversible drying agent⁵¹ that forms phosphoric acid upon reaction with water. Suspended above the reaction, this reagent trapped the water evolved from acetal formation and thus helped to drive the polymerization. GPC analysis of the polymers revealed that the phosphorus pentoxide successfully increased molecular weight but still, yields and molecular weights generally decreased in proportion to the amount of erythritol in the copolymerization feed for each series: **E/P-VV** (Table I); **E/D-VV** (Table II); **E/P-SS** (Table III); and **E/D-SS** (Table IV). Note that other factors impact the isolated yield. Thus, polymer solubility, precipitation phenomena, and transfer yield can generate exceptions to the yield trends. Still, for each copolymer series, erythritol feeds > 70% invariably gave lower polymer yields than erythritol feeds < 30%.

For each copolymer series, Figure 2 illustrates that the erythritol incorporation fraction is universally less than the feed fraction. For low **E** feed fractions (10–20%), incorporation of erythritol was minimal: 6–9% with **VV** and 0–6% with **SS**. In these cases, the amount of erythritol present is small enough for the polymerization to occur with the more reactive **P** or **D**, excluding **E**. With a feed of 40% **E**, the average erythritol incorporation is about 25%. With a feed of 60% **E**, the average erythritol incorporation is about 44%. The maximum **E** incorporation achieved was 86% for **E/D-SS**—only 4% below the **E** feed of 90%.

Polymer Thermal Properties

As shown in Tables I–IV, the obtained polyacetals are generally amorphous. The two exceptions are **E/P-VV** (Table I) made

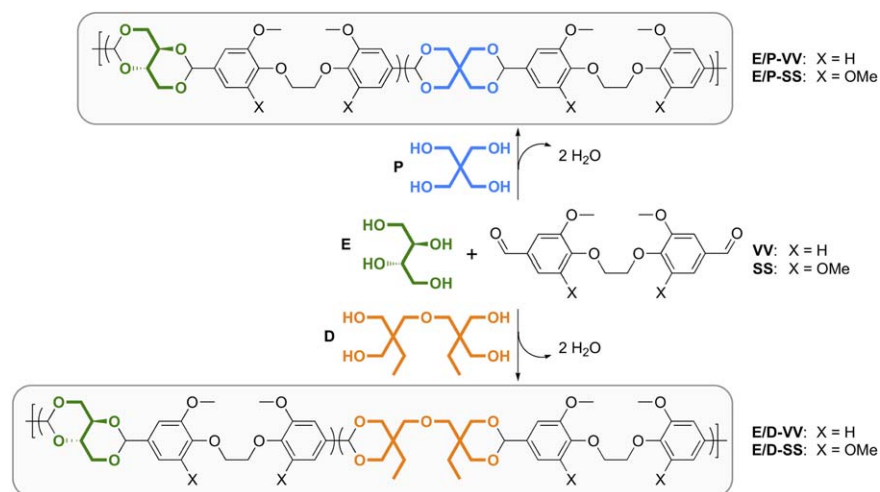


Figure 1. Polyacetal copolymers (E/P-VV, E/P-SS, E/D-VV, and E/D-SS) are synthesized by the condensation polymerization of bioaromatic dialdehydes (VV or SS) with erythritol (E) along with another tetraol, pentaerythritol (P), or ditrimethylolpropane (D). [Color figure can be viewed in the online issue, which is available at wileyonlinelibrary.com.]

with 80 and 90% erythritol feeds which show melting temperatures of 166 and 159 °C, respectively. However, it should be noted that these samples are also the two lowest molecular weight polymers and the melting temperatures, thus, could just be related to crystallization of specific oligomers present in the sample. And, to the extent that polymer crystallization is kinetically slow with long, rigid polymers, lower molecular weight samples—with ample free volume—may happen to crystallize during the timescale of the DSC experiment. This matches our previous results²⁷ suggesting that polymers made from tetraols D and P and dialdehydes VV and SS are generally amorphous. As elaborated below, enchainment of erythritol does not yield a stereoregular polymer and thus, the amorphous character of E-VV and E-SS is predicted.

The 100% erythritol polymer derived from syringaldehyde (E-SS) has a glass transition temperature (T_g) of 135 °C. This is considerably higher than the T_g value of 74 °C for the 100% erythritol polymer derived from vanillin (E-VV). In fact, a general observation is that the SS polymers exhibit higher glass transition temperatures than the VV polymers. Figure 3 plots the T_g values for the four copolymer series investigated. The syringaldehyde-based copolymers show a higher T_g range (71–159 °C) than the vanillin-based copolymers (57–110 °C). The additional methoxy group of the syringaldehyde units presumably increases conformational barriers and thereby increases T_g . This effect agrees with T_g values we have previously measured for polyacetals based on VV and SS,²⁷ but is opposite that observed for polyalkylene vanillate and polyalkylene syringate

Table I. Thermal and Molecular Weight Data for the E/P-VV Copolymer Series from Erythritol (E)/Pentaerythritol (P) and the Dialdehyde VV^a

Entry	Tetraol feed % ^b		Inc. E ^b (%)	Yield (%)	M_n^c (Da)	M_w^c (Da)	PDI ^c	T_g^d (°C)	T_{95}^e (°C)
	HO-CH ₂ -CH(OH)-CH ₂ -OH	HO-CH ₂ -C(OH)(CH ₂ -OH) ₃							
1	0	100	0	84.8	6,400	11,500	1.8	100	307
2	20	80	9	52.0	7,700	15,800	2.1	110	315
3	40	60	16	77.2	3,500	6,800	1.9	96	290
4	50	50	34	84.1	3,700	7,600	2.0	87	304
5	60	40	43	90.6	3,900	8,500	2.2	97	302
6	80	20	34	42.1	1,400	2,300	1.7	67	249
7	90	10	71	47.1	1,700	2,700	1.6	58	251
8	100	0	100	46.1	2,900	6,300	2.1	74	275

^aPolymerization conducted in refluxing methylene chloride at 40 °C for 48 h; 1 mol % *p*-TSA.

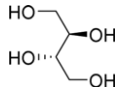
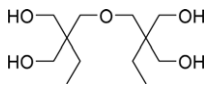
^bTetraol feed and incorporation are expressed in mol %. Incorporation of erythritol (E) and pentaerythritol (P) in the copolymers was determined by integration of respective acetal peak in ¹H NMR.

^cMolecular weight data obtained by GPC in HFIP at 40 °C versus PMMA standards.

^dDetermined by DSC. Entries 6 and 7 presented T_m endotherms at 166 and 159 °C, respectively.

^eTemperature reported upon 5% mass loss.

Table II. Thermal and Molecular Weight Data for the **E/D-VV** Copolymer Series from Erythritol (**E**)/Ditrimethylolpropane (**D**) and the Dialdehyde **VV**^a

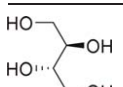
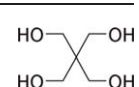
Entry	Tetraol feed (%) ^b		Inc. E ^b (%)	Yield (%)	M_n^c (Da)	M_w^c (Da)	PDI ^c	T_g^d (°C)	T_{95}^e (°C)
									
9	0	100	0	92.6	11,300	24,200	2.1	73	318
10	20	80	6	90.0	8,100	17,600	2.2	73	310
11	40	60	28	96.1	10,700	22,100	2.1	76	313
12	50	50	31	76.2	3,600	7,100	2.0	65	295
13	60	40	33	86.0	2,400	4,200	1.8	57	279
14	80	20	73	74.1	2,400	4,900	2.0	75	291
15	90	10	76	55.0	3,200	7,000	2.2	64	285
8	100	0	100	46.1	2,900	6,300	2.1	74	275

^aPolymerization conducted in refluxing methylene chloride at 40 °C for 48 h; 1 mol % *p*-TSA.^bTetraol feed and incorporation are expressed in mol %. Incorporation of erythritol (**E**) and ditrimethylolpropane (**D**) in the copolymers was determined by integration of respective acetal peak in ¹H NMR.^cMolecular weight data obtained by GPC in HFIP at 40 °C versus PMMA standards.^dDetermined by DSC.^eTemperature reported upon 5% mass loss.

polymers, for which the additional methoxy group lowers the T_g modestly.³⁷ A final trend revealed in Figure 3 is that the ditrimethylolpropane (**D**) segment imparts a lower glass transition temperature compared to analogous polymers bearing pentaerythritol (**P**). This is expected when considering the conformational flexibility of **D** versus the conformational rigidity of the spiro bicyclic structure formed with **P**.

The T_g values exhibited by this polymer series span those provided by several common commodity plastics, such as PET³³ and PS.¹² At the same time, the thermal properties can be tuned depending on the erythritol (**E**) feed, the nature of the dialdehyde, and the balance tetraol. The T_g values match or exceed those of many other bioaromatic polymers, such as the polyester reported from the condensation of dimethyl

Table III. Thermal and Molecular Weight Data for the **E/P-SS** Copolymer Series from Erythritol (**E**)/Pentaerythritol (**P**) and the Dialdehyde **SS**^a

Entry	Tetraol feed (%) ^b		Inc. E ^b (%)	Yield (%)	M_n^c (Da)	M_w^c (Da)	PDI ^c	T_g^d (°C)	T_{95}^e (°C)
									
16	0	100	0	88.7	21,900	38,700	1.8	159	265
17	10	90	2	86.8	27,100	46,800	1.7	127	276
18	20	80	2	83.5	11,100	17,900	1.6	109	248
19	30	70	16	92.9	13,400	27,000	2.0	85	237
20	40	60	34	82.6	9,500	18,100	1.9	121	298
21	50	50	36	82.0	13,100	22,800	1.7	89	267
22	60	40	51	76.7	10,100	18,800	1.9	82	296
23	70	30	58	69.4	6,900	12,700	1.8	96	231
24	80	20	62	69.4	6,300	11,600	1.9	94	210
25	90	10	76	79.5	7,100	13,000	1.8	98	281
26	100	0	100	28.4	7,800	15,300	2.0	135	256

^aPolymerization conducted in refluxing methylene chloride at 40 °C for 48 h; 1 mol % *p*-TSA.^bTetraol feed and incorporation are expressed in mol %. Incorporation of erythritol (**E**) and pentaerythritol (**P**) in the copolymers was determined by integration of respective acetal peak in ¹H NMR.^cMolecular weight data obtained by GPC in HFIP at 40 °C versus PMMA standards.^dDetermined by DSC.^eTemperature reported upon 5% mass loss.

Table IV. Thermal and Molecular Weight Data for the E/D-SS Copolymer Series from Erythritol (E)/Ditrimethylolpropane (D) and the Dialdehyde SS^a

Entry	Tetraol feed (%) ^b		Inc. E ^b (%)	Yield (%)	M_n^c (Da)	M_w^c (Da)	PDI ^c	T_g^d (°C)	T_{95}^e (°C)
	Erythritol	Ditrimethylolpropane							
27	0	100	0	73.7	14,800	24,200	1.6	93	297
28	10	90	6	98.9	19,200	34,300	1.8	91	313
29	20	80	0	99.0	20,400	36,300	1.8	92	312
30	30	70	13	92.2	15,000	27,100	1.8	95	305
31	40	60	24	92.0	15,900	31,400	2.0	101	312
32	50	50	41	94.0	18,800	37,700	2.0	103	312
33	60	40	47	64.7	8,600	17,100	2.0	82	285
34	70	30	52	55.6	7,100	12,900	1.8	92	295
35	80	20	58	52.9	3,300	5,500	1.7	74	256
36	90	10	86	57.0	6,300	10,900	1.7	71	248
26	100	0	100	28.4	7,800	15,300	2.0	135	256

^aPolymerization conducted in refluxing methylene chloride at 40 °C for 48 h; 1 mol % *p*-TSA.

^bTetraol feed and incorporation are expressed in mol %. Incorporation of erythritol (E) and ditrimethylolpropane (D) in the copolymers was determined by integration of respective acetal peak in ¹H NMR.

^cMolecular weight data obtained by GPC in HFIP at 40 °C versus PMMA standards.

^dDetermined by DSC.

^eTemperature reported upon 5% mass loss.

succinate and methylated/reduced bis-vanillin, which bears a T_g of 68 °C.³⁹

Erythritol Acetal Structure Analysis

Unlike pentaerythritol (P) and ditrimethylolpropane (D), erythritol can form a cyclic acetal in three distinct modes. Figure 4(a) shows the three possible structures: a 1,2:3,4 bis-acetal forming linked five-membered rings (I); a 1,3:2,4 bis-acetal forming fused six-membered rings (II); and a 1,4:2,3 bis-acetal forming a fused five/seven ring system (III). In order to investigate the preferred mode of enchainment, a model compound (BEB) was

synthesized from two equivalents of benzaldehyde (B) and erythritol (E). Solution ¹H-NMR analysis of BEB showed a single acetal proton (5.78 ppm). This single acetal resonance suggests that a single isomer is present in solution and discounts the unsymmetrical, fused five/seven ring system (III) because its acetal protons are inequivalent. Computational determination of the heats of formation (Spartan '10, T1 Thermochemical Recipe) of the 1,2:3,4 bis-acetal (I) and the 1,3:2,4 bis-acetal (II) showed that the fused ring system (II) is lower in energy by 3.35 kcal/mol.⁵² Single crystals of BEB, suitable for X-ray analysis, were grown from a slowly-evaporating solution in THF. Figure 4(b) shows

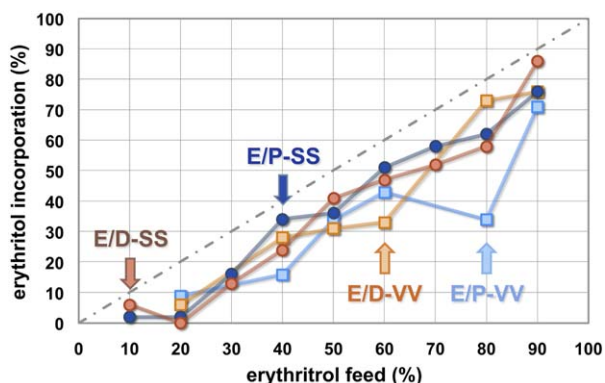


Figure 2. The erythritol incorporation fraction is generally proportional to the feed fraction for all four copolymer series (E/P-VV, E/D-VV, E/P-SS, and E/D-SS). That the incorporation is always less than the feed highlights the reluctance of erythritol (E) to polymerize vs. the competing tetraol, pentaerythritol (P) or ditrimethylolpropane (D). [Color figure can be viewed in the online issue, which is available at wileyonlinelibrary.com.]

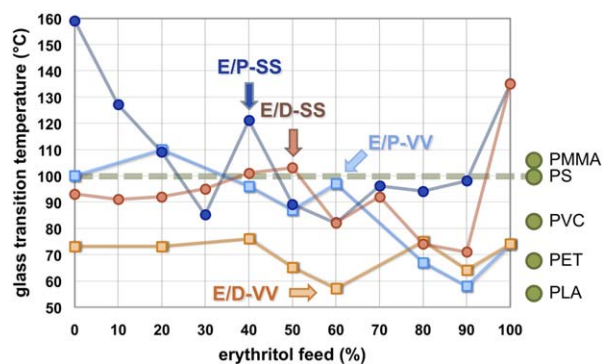


Figure 3. For the copolymer series E/P-VV, E/D-VV, E/P-SS, and E/D-SS, the glass transition temperature is modestly affected by the erythritol (E) content. More importantly, the SS unit (from syringaldehyde) confers a greater T_g than the VV unit (from vanillin), while the E/P series show higher T_g values than the E/D series. Several polymers show T_g values competitive with commodity plastics, including the key threshold of 100 °C for PS.¹² [Color figure can be viewed in the online issue, which is available at wileyonlinelibrary.com.]

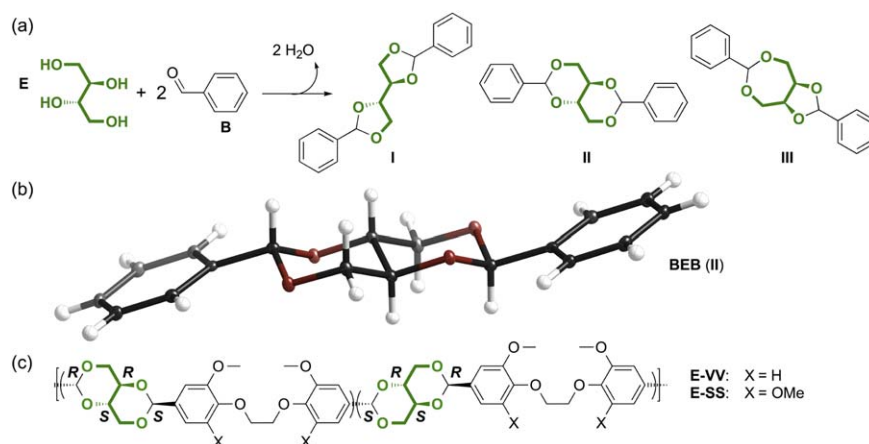


Figure 4. (a) Bis-acetal formation from erythritol (E) and benzaldehyde (B) can result in three modes of connectivity: a 1,2:3,4 bis-acetal with linked rings (I); a symmetrical 1,3:2,4 bis-acetal with fused rings (II); and an unsymmetrical 1,4:2,3 bis-acetal with fused rings (III). (b) Solid state X-ray crystal structure analysis of BEB (shown with 50% probability ellipsoids) reveals that the symmetrical fused ring system (II) prevails. (c) The E-VV and E-SS polymers are likely atactic because the erythritol segment can begin with either R or S stereochemistry. This structure has been submitted to the Cambridge Crystallographic Data Centre and assigned #1476724. [Color figure can be viewed in the online issue, which is available at wileyonlinelibrary.com.]

the crystal structure revealed by the X-ray study. It is clearly the 1,3:2,4 bis-acetal (II) with the fused ring connection, as suggested by solution NMR and the computational analysis. This *trans* stereoisomer is C_i -symmetric and thus is achiral and possesses an inversion center. Such stereochemistry is expected because erythritol itself is an achiral meso (*R,S*) compound. To better understand the stereochemistry concerning the erythritol enchainment, model compounds analogous to BEB were synthesized from vanillin (VEV) and syringaldehyde (SES). For both VEV and SES, ^1H NMR shows a major peak near 5.65 ppm for the acetal hydrogen, but also a minor acetal peak near 5.81 ppm, suggesting multiple modes of erythritol enchainment (*trans* and *cis*) and the likely outcome that the E-VV and E-SS polymers are atactic. Moreover, Figure 4(c) shows that the RRSS stereocenters of a *trans* erythritol segment can be incorporated in either the forward or reverse direction. The likely lack of stereoselectivity during the polymerization yields a polymer with insufficient stereoregularity to crystallize. This presumably explains the absence of a melting temperature for the E-VV or E-SS polymers.

NMR Analysis of Erythritol Incorporation

To calculate the incorporation of erythritol (E) into the polymers, a detailed NMR analysis was performed on the copolymer sample E/P-SS with 50%E/50%P. It was found by analyzing the acetal region that three peaks of distinctly different integrations were observed—in contrast to the P-SS polymer, for which there is only one peak and the E-SS polymer, for which there are two peaks. The E/P-SS sample was subjected to extensive 2D NMR analysis at 75 °C (a detailed report can be found in the Supporting Information). It was determined that the peak at 5.44 ppm corresponds to the acetal proton formed with P, whereas the peaks at 5.72 and 5.89 ppm represent stereoisomeric forms of enchainment E. The peak at 5.72 ppm contains the acetal hydrogens of both the equatorial/equatorial (*trans*) and axial/equatorial (*cis*) stereoisomers. [See BEB of Figure 4(b), which shows the equatorial/equatorial analogue.] However, the peak at 5.89 ppm represents the axial/axial (conformational)

stereoisomer, which is less abundant because of sterically unfavorable 1,3-diaxial interactions. With these assignments, it was possible to calculate the polymeric abundance of E versus P by comparing the integration of the aforementioned peaks. It should be noted that this NMR analysis exhibits some inherent variation. For example, the quantification of the E50/P50-SS polymer at 75 °C indicated a 44% E incorporation with spectrum deconvolution. The same polymer analyzed at 25 °C with poorer peak resolution and no deconvolution indicated a 36% E incorporation. Thus, there seems to be a variation of at least 8% depending on the method.

Preliminary Degradation Studies

A simple study of degradation was performed by reanalyzing the GPC polymer samples 24 h after their dissolution in the GPC solvent, HFIP. This solvent is considerably acidic ($pK_a = 9.3$)^{53,54} and thus can promote the acid-catalyzed hydrolysis of the polyacetals with adventitious water (or possibly transacetalization with HFIP itself). The number average molecular weight (M_n) of the polymers decreased dramatically in all samples, ranging from 10% to more than 80%, but above a 50% decrease in the majority of cases. The E/P-SS series showed the least degradation, averaging an M_n loss below 30%. However, polymers containing VV showed the greatest degradation, with an average M_n loss around 60% for both series. These results seem to correlate with the initial M_n ; that is, the E/P-SS series had the highest initial M_n and hydrolyzed less, whereas the VV series had lower initial M_n and showed more advanced degradation. The tetraol comonomers P and D were seemingly interchangeable regarding their impact on degradation. Finally, the 100% erythritol polymers E/VV and E/SS were the most resistant to degradation, with M_n losses of only 10.3 and 11.5%, respectively.

Additional, heterogeneous degradation studies were conducted by agitating a sample from each series (E60/P40-VV from Table I, entry 5; E40/D60-VV from Table II, entry 11; E50/P50-SS from Table III, entry 21; and E50/D50-SS from Table IV, entry

32) in either 3, 6, or 12 M (concentrated) aqueous HCl for 24 h. In 3 M aqueous HCl, degradation was incomplete, with both polymer and hydrolyzed monomer observed in the HFIP GPC chromatograms (see the Supporting Information). The M_n loss was greater for samples containing P, rather than D: E60/P40-VV lost 49% (3,900 to 2,000) and E50/P50-SS lost 53% (13,100 to 6,100). In 6 M aqueous HCl, the samples completely hydrolyzed to monomer, except for E40/D60-VV, for which M_n loss was only 56% (10,700 to 4,700). In concentrated aqueous HCl, all four samples were completely hydrolyzed to monomer. These results clearly indicate the facile hydrolysis degradation of these polymers when in contact with acidic media.

Finally, a long-term degradation study was conducted with E50/D50-SS. Over a period of one year, 10 mg samples were agitated with an orbital shaker in the following aqueous environments: seawater, deionized water, tap water, pH 5 buffer, or pH 1 buffer (10 mL each). Visual inspection and GPC analysis indicated essentially no change in the first four samples; no decrease in the M_n value was observed. However, under pH 1 conditions, the solid sample partially disintegrated and yielded a cloudy suspension (see photographs in the Supporting Information). This sample was subjected to GPC analysis, which showed a small, broad peak with $M_n = 11,200$ and PDI = 2.7. This amounts to a 40% decrease in the M_n (initially 18,800) and a slight broadening of the PDI (initially 2.0). The major peak of the chromatogram corresponded to monomer ($M_n = 600$). Overall, this long-term study indicates that bioaromatic polyacetals can have appreciable lifetime in various aqueous environments, but will eventually yield to degradation via acid-catalyzed hydrolysis. Additional degradation studies are ongoing that better mimic realistic environmental conditions.

CONCLUSIONS

Erythritol, a naturally occurring carbohydrate derivative, was used for the first time to prepare biorenewable polyacetals. Erythritol is of special interest since it is a non-toxic, biogenic molecule available in large, sustainable quantities via glucose fermentation. This tetraol was polymerized with dialdehydes prepared from the bioaromatics vanillin and syringaldehyde, both abundantly available from lignin. Erythritol polymerization was enhanced via copolymerization with other tetraols (pentaerythritol and ditrimethylolpropane) having greater reactivity. The polyacetals could be obtained with high molecular weight and generally exhibited high glass transition temperatures competitive with those of several commercial, commodity plastics. For example, E-SS, derived from erythritol and syringaldehyde, has a T_g of 135 °C, substantially higher than that of PS (100 °C). Preliminary, heterogeneous degradation studies in an acidic aqueous media showed facile degradation proportional to the HCl concentration (3 M, 6 M, concentrated). A one-year experiment showed that E50/D50-SS is not substantially degraded by seawater, deionized water, tap water, or pH 5 buffer, but is 40% degraded by pH 1 buffer. Additional investigation of these aromatic polyacetals is required to further optimize their synthesis by using more environmentally friendly solvents and seeking even higher molecular weights for the polymers with high erythritol content. More elaborate degradation studies are

required to better understand the degradation mechanism, products, kinetics, and feasibility under realistic environmental conditions.

ACKNOWLEDGMENTS

This research was supported by the National Science Foundation (CHE-0848236 and CHE-1305794) and the University of Florida. KAA wishes to acknowledge the National Science Foundation (CHE-0821346) and the University of Florida for funding of the purchase of the X-ray equipment.

REFERENCES

1. U.S. Energy Information Administration. Do We Have Enough Oil Worldwide to Meet Our Future Needs? Available at: <https://www.eia.gov/tools/faqs/faq.cfm?id=38&t=6>, 2014.
2. Worldwatch Institute. Global Plastic Production Rises, Recycling Lags, Available at: <http://www.worldwatch.org/global-plastic-production-rises-recycling-lags-0>, 2015.
3. Anastas, P. T.; Warner, J. C. *Green Chemistry: Theory and Practice*; Oxford University Press: New York, 1998; Chapter 4, p 30.
4. Wool, R. American Chemical Society, Green Chemistry Principle #7: Use of Renewable Feedstocks, Available at: <https://www.acs.org/content/acs/en/greenchemistry/what-is-green-chemistry/principles/green-chemistry-principle-7.html>.
5. Garlotta, D. J. *Polym. Environ.* 2002, 9, 63.
6. Drumright, R. E.; Gruber, P. R.; Henton, D. E. *Adv. Mater.* 2000, 12, 1841.
7. Dechy-Cabaret, O.; Martin-Vaca, B.; Bourissou, D. *Chem. Rev.* 2004, 104, 6147.
8. Vink, E. T. H.; Rabago, K. R.; Glassner, D. A.; Springs, B.; O'Conner, R. P.; Kolstad, J.; Gruber, P. R. *Macromol. Biosci.* 2004, 4, 551.
9. Mehta, R.; Kumar, V.; Bhunia, H.; Upadhyay, S. N. *J. Macromol. Sci. Polym. Rev.* 2005, 45, 325.
10. Markets and Markets. Polyolefins Market Consumption Worth 169,892.4 Kilotons by 2018, Available at: <http://www.marketsandmarkets.com/PressReleases/polyolefins.asp>, 2015.
11. Aou, K.; Kang, S.; Hsu, S. L. *Macromolecules* 2005, 38, 7730.
12. Priddy, D. B. Kirk-Othmer Encyclopedia of Chemical Technology; Wiley: New York, 2006; Vol. 23, pp 358–416.
13. Jacobsen, A.; Fritz, H. G. *Polym. Eng. Sci.* 1999, 39, 1303.
14. Drieskens, M.; Peeters, R.; Mullens, J.; Franco, D.; Lemstra, P. J.; Hristova-Bogaerds, D. G. *J. Polym. Sci.: Part B: Polym. Phys.* 2009, 47, 2247.
15. Sinclair, R. G. *J. Macromol. Sci. Part A: Pure Appl. Chem.* 1996, A33, 585.
16. Rudeekit, Y.; Numnoi, J.; Tajan, M.; Chaiwutthinan, P.; Leejarkpai, T. *J. Met. Mater. Miner.* 2008, 18, 83.
17. Kijchavengkul, T.; Aurus, R. *Polym. Int.* 2008, 57, 793.
18. Royte, E. Corn Plastic to the Rescue, Smithsonian Magazine; Available at: <http://www.smithsonianmag.com/science-nature/plastic.html>. 2006; pp 84–88. Accessed July 2016.

19. Natureworks PLA Composting: "End Products Made With 100% Ingeo Will Compost in Municipal/Industrial Facilities According to ISO, ASTM, and EN regulations, and Ingeo is Certified Appropriately. The number of These Facilities are Limited and May Not be Available Near You." Available at: <http://www.natureworkslc.com/The-Ingeo-Journey/End-of-Life-Options/Composting>.
20. Kunioka, M.; Ninomiya, F.; Funabashi, M. *Polym. Degrad. Stabil.* **2006**, *91*, 1919.
21. Bukhamseen, F.; Novotny, L. *Res. J. Pharm. Biol. Chem. Sci.* **2014**, *5*, 638.
22. U.S. Food and Drug Administration. Agency Response Letter GRAS Notice No. GRN 000076, Available at: <http://www.fda.gov/downloads/Food/IngredientsPackagingLabeling/GRAS/NoticeInventory/UCM266643>, **2001**.
23. Kobben, S.; Ethirajan, A.; Junkers, T. J. *Polym. Sci. Part A: Polym. Chem.* **2014**, *52*, 1633.
24. Teng, L.; Nie, W.; Zhou, Y.; Chen, P. *Polym. Bull.* **2016**, *73*, 97.
25. Bueno, M.; Molina, M.; Galbis, J. A. *Polym. Degrad. Stabil.* **2012**, *97*, 1662.
26. Barrett, D. G.; Luo, W.; Yousaf, M. N. *Polym. Chem.* **2010**, *1*, 296.
27. Pemba, A. G.; Rostagno, M.; Lee, T. A.; Miller, S. A. *Polym. Chem.* **2014**, *5*, 3214.
28. Lebo, S. E. Jr.; Gargulak, J. D.; McNally, T. J. *Kirk-Othmer Encyclopedia of Chemical Technology*; Wiley: New York, **2001**; Vol. 15, pp 1–32.
29. Fache, M.; Boutevin, B.; Caillol, S. *ACS Sust. Chem. Eng.* **2016**, *4*, 35.
30. Wu, G.; Heitz, M.; Chornet, E. *Ind. Eng. Chem. Res.* **1994**, *33*, 718.
31. Brebu, M.; Vasile, C. *Cell. Chem. Technol.* **2010**, *44*, 353.
32. Wong, Z.; Chen, K.; Li, J. *Bioresources* **2010**, *3*, 1509.
33. East, A. J. *Kirk-Othmer Encyclopedia of Chemical Technology*; Wiley: New York, **2006**; Vol. 20, pp 31–95.
34. Fache, M.; Darroman, E.; Besse, V.; Rémi, A.; Caillol, S.; Boutevin, B. *Green Chem.* **2014**, *16*, 1987.
35. Holmberg, A. L.; Stanzione, J. F.; Wool, R. P.; Epps, T. H. *ACS Sust. Chem. Eng.* **2014**, *2*, 569.
36. Liu, H.; Lepoittevin, B.; Roddier, C.; Guerineau, V.; Bech, L.; Herry, J.; Bellon-Fontaine, M.; Roger, P. *Polymer* **2011**, *52*, 1908.
37. Mialon, L.; Vanderhenst, R.; Pemba, A. G.; Miller, S. A. *Macromol. Rapid Commun.* **2011**, *32*, 1386.
38. Amarasekara, A. S.; Razzaq, A. *ISRN Polym. Sci.* **2012**, *2012*, 1.
39. Llevot, A.; Grau, E.; Carlotti, S.; Grelier, S.; Cramail, H. *Polym. Chem.* **2015**, *6*, 6058.
40. Llevot, A.; Grau, E.; Carlotti, S.; Grelier, S.; Cramail, H. *Polym. Chem.* **2015**, *6*, 7693.
41. Firdaus, M.; Meier, M. A. R. *Eur. Polym. J.* **2013**, *49*, 156.
42. Pang, C.; Zhang, J.; Wu, G.; Wang, Y.; Gaob, H.; Ma, J. *Polym. Chem.* **2014**, *5*, 2843.
43. Harvey, B. G.; Guenther, A. J.; Meylemans, H. A.; Haines, S. R. L.; Lamison, K. R.; Groshens, T. J.; Cambrea, L. R.; Davisa, M. C.; Lai, W. W. *Green Chem.* **2015**, *17*, 1249.
44. Fache, M.; Boutevin, B.; Caillol, S. *Eur. Polym. J.* **2015**, *68*, 488.
45. Llevot, A.; Grau, E.; Carlotti, S.; Grelier, S.; Cramail, H. *Macromol. Rapid Commun.* **2016**, *37*, 9.
46. Pemba, A. G.; Flores, J. A.; Miller, S. A. *Green Chem.* **2013**, *15*, 325.
47. Chikkali, S.; Stempfle, F.; Mecking, S. *Macromol. Rapid Commun.* **2012**, *33*, 1126.
48. Rajput, B. S.; Gaikwad, S. R.; Menon, S. K.; Chikkali, S. H. *Green Chem.* **2014**, *16*, 3810.
49. Lingier, S.; Espeel, P.; Suarez Suarez, S.; Türünç, O.; De Wildeman, S.; Du Prez, F. E. *Eur. Polym. J.* **2015**, *70*, 232.
50. Luebben, S. D.; Raebiger, J. W. In *A Novel Renewable Thermoplastic Polyacetal by Polymerization of Glycolaldehyde Dimer, a Major Product of the Fast Pyrolysis of Cellulosic Feedstock ACS Symposium Series*; Cheng, H. N., Gross, R. A., Smith, P. B., Eds.; Green Polymer Chemistry III: Biobased Materials and Biocatalysis; **2015**; Vol. 1192, Chapter 19, p 305.
51. Burfield, D. R.; Lee, K.; Smithers, R. H. *J. Org. Chem.* **1977**, *42*, 3060.
52. Pemba, A. G. *Polyacetals from Bioderived Starting Materials as Potential Replacements for Commodity Packaging Plastics*; Ph.D. Dissertation, University of Florida, **2014**.
53. Bordwell, F. G. *Acc. Chem. Res.* **1988**, *21*, 456.
54. Hinou, H.; Hyugaji, K.; Garcia-Martin, F.; Nishimura, S. I.; Albericio, F. *RSC Adv.* **2012**, *2*, 2729.